

# [2+3] Cycloaddition of Ethylene to Transition Metal Oxo Compounds. Analysis of Density Functional Results by Marcus Theory

Philip Gisdakis and Notker Rösch\*

Contribution from the Institut für Physikalische und Theoretische Chemie, Technische Universität München, 85747 Garching, Germany

Received July 20, 2000. Revised Manuscript Received November 9, 2000

**Abstract:** Density functional results on the [2+3] cycloaddition of ethylene to various transition metal complexes  $\text{MO}_3^q$  and  $\text{LMO}_3^q$  ( $q = -1, 0, 1$ ) with  $M = \text{Mo, W, Mn, Tc, Re, and Os}$  and various ligands  $L = \text{Cp, CH}_3, \text{Cl, and O}$  show that the corresponding activation barriers  $\Delta E^\ddagger$  depend in quadratic fashion on the reaction energies  $\Delta E_0$  as predicted by Marcus theory. A thermoneutral reaction is characterized by the intrinsic reaction barrier  $\Delta E_0^\ddagger$  of 25.1 kcal/mol. Both ethylene [2+3] cycloaddition to an oxo complex and the corresponding homolytic M–O bond dissociation are controlled by the reducibility of the transition metal center. Indeed, from the easily calculated M–O bond dissociation energy of the oxo complex one can predict the reaction energy  $\Delta E_0$  and hence, by Marcus theory, the corresponding activation barrier  $\Delta E^\ddagger$ . This allows a systematic representation of more than 25 barriers of [2+3] cycloaddition reactions that range from 5 to 70 kcal/mol.

## 1. Introduction

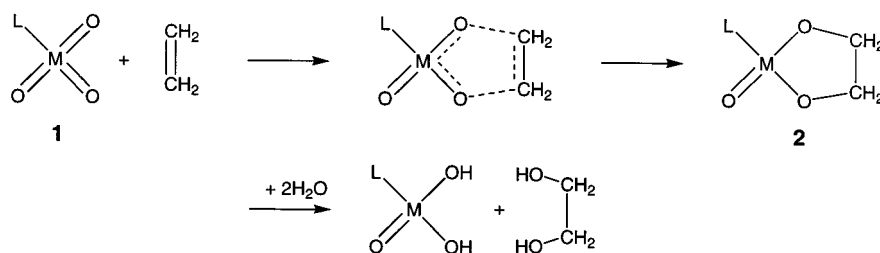
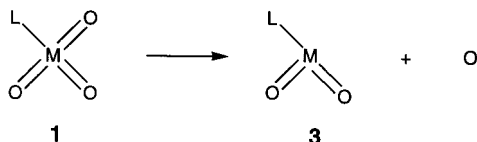
Dihydroxylation of olefins is an important class of oxygen transfer reactions mediated by transition metal oxo compounds.<sup>1–3</sup> Recently, many experimental and theoretical investigations have focused on mechanistic aspects of this type of reaction. Theoretical studies of olefin dihydroxylation catalyzed by complexes of the type  $\text{LMO}_3$  **1** ( $M = \text{Os, Ru, Mn, Cr}$ ) revealed significant mechanistic details.<sup>4–12</sup> In epoxidation reactions, the metal complex reacts first with an oxygen source to form a peroxo (e.g., in the system methyltrioxorhenium/ $\text{H}_2\text{O}_2$ )<sup>13–18</sup> or a hydroperoxo species (in case of titanium and molybdenum complexes),<sup>19–21</sup> which in turn transfers an oxygen atom to the olefin. In the first step of the dihydroxylation reaction catalyzed

by transition metal oxo compounds such as  $\text{OsO}_4$ ,<sup>1–3</sup> the olefin reacts directly with a  $\text{O}=\text{M}=\text{O}$  unit in a [2+3] manner to form a dioxylate<sup>22</sup> (see Scheme 1). The previously suggested [2+2] pathway<sup>23</sup> was ruled out, at least for  $\text{OsO}_4$ , by density functional (DF) calculations,<sup>4–6</sup> partly combined with measurements of kinetic isotope effects.<sup>7</sup> Recently, both pathways were analyzed for some compounds of the type  $\text{LReO}_3$ .<sup>24,25</sup> Pietsch et al.<sup>24</sup> compared the [2+2] and [2+3] pathways by focusing only on the formation energy of the metallaioxetane and the metalla-dioxolane intermediate **2**; they contended that the  $\pi$  donor strength of the ligands  $L$  is responsible for the reactivity differences of this type of complexes. To corroborate these selection arguments Deubel and Frenking<sup>25</sup> additionally determined the reaction barriers of both reactions as well as the barrier of the rearrangement of the intermediate to the dioxylate. From their results one notes that for all complexes  $\text{LReO}_3$  ( $L = \text{O}^-, \text{Cl, Cp}$ ) the [2+2] pathway features a higher barrier than the corresponding [2+3] pathway; furthermore, barriers of the rearrangement reaction, which follows the [2+2] cycloaddition and leads to the dioxylate, were calculated higher yet. Deubel and Frenking<sup>25</sup> rationalized the reactivity differences using a charge-transfer model and a frontier orbital argument.

With the present DF study<sup>26</sup> we intend to explore the mechanism of the [2+3] cycloaddition for a wide variety of transition metal oxo complexes **1** (see Scheme 1). We will compare reaction energies, activation barriers, and transition state geometries with the aim of identifying molecular properties that determine the reactivity of these complexes. We will proceed in two steps. First, with the help of Marcus theory,<sup>36</sup>

- (1) Kolb, H. C.; VanNieuwenzhe, M. S.; Sharpless, K. B. *Chem. Rev.* **1994**, *94*, 2483.
- (2) Johnson, R. A.; Sharpless, K. B. In *Catalytic Asymmetry Synthesis*; Ojima, J., Ed.; VCH: Weinheim, 1993; p 227.
- (3) Schröder, M. *Chem. Rev.* **1980**, *80*, 187.
- (4) Dapprich, S.; Ujaque, G.; Maseras, F.; Lledos, A.; Musaev, D. G.; Morokuma, K. *J. Am. Chem. Soc.* **1996**, *118*, 11660.
- (5) Pidun, U.; Boehme, C.; Frenking, G. *Angew. Chem., Int. Ed. Engl.* **1996**, *35*, 2817.
- (6) Torrent, M.; Deng, L.; Duran, M.; Sola, M.; Ziegler, T. *Organometallics* **1997**, *16*, 13.
- (7) DelMonte, A. J.; Haller, J.; Houk, K. N.; Sharpless, K. B.; Singleton, D. A.; Strassner, T.; Thomas, A. A. *J. Am. Chem. Soc.* **1997**, *119*, 9907.
- (8) Nelson, D. W.; Gypser, A.; Ho, P. T.; Kolb, H. C.; Kondo, T.; Kwong, H.; McGrath, D. V.; Rubin, A. E.; Norrby, P.; Gable, K. P.; Sharpless, K. B. *J. Am. Chem. Soc.* **1997**, *119*, 1840.
- (9) Corey, E. J.; Noe, M. C. *J. Am. Chem. Soc.* **1996**, *118*, 319.
- (10) Haller, J.; Strassner, T.; Houk, K. N. *J. Am. Chem. Soc.* **1997**, *119*, 8031.
- (11) Houk, K. N.; Strassner, T. *J. Org. Chem.* **1999**, *64*, 800.
- (12) Torrent, M.; Deng, L.; Ziegler, T. *Inorg. Chem.* **1998**, *37*, 1307.
- (13) Herrmann, W. A. *J. Organomet. Chem.* **1995**, *500*, 149.
- (14) Herrmann, W. A.; Kühn, F. E. *Acc. Chem. Res.* **1997**, *30*, 169.
- (15) Romão, C. C.; Kühn, F. E.; Herrmann, W. A. *Chem. Rev.* **1997**, *97*, 3197.
- (16) Herrmann, W. A.; Fischer, R. W.; Scherer, W.; Rauch, M. U. *Angew. Chem., Int. Ed. Engl.* **1993**, *32*, 1157.
- (17) Al-Ajlouni, A. M.; Espenson, J. H. *J. Am. Chem. Soc.* **1995**, *117*, 9243.
- (18) Al-Ajlouni, A. M.; Espenson, J. H. *J. Org. Chem.* **1996**, *61*, 3969.

- (19) Wu, Y.; Lai, D. K. W. *J. Org. Chem.* **1995**, *60*, 673.
- (20) Thiel, W. R. *Chem. Ber.* **1996**, *129*, 575.
- (21) Thiel, W. R. *J. Mol. Catal. A* **1997**, *117*, 449.
- (22) Criegee, R. *Liebigs Ann. Chem.* **1936**, *522*, 75.
- (23) Sharpless, K. B.; Teranishi, A. Y.; Bäckvall, J.-E. *J. Am. Chem. Soc.* **1977**, *99*, 3120.
- (24) Pietsch, M. A.; Russo, T. V.; Murphy, R. B.; Martin, R. L.; Rappé, A. K. *Organometallics* **1998**, *17*, 2716.
- (25) Deubel, D. V.; Frenking, G. *J. Am. Chem. Soc.* **1999**, *121*, 2021.

**Scheme 1.** [2+3] Cycloaddition**Scheme 2.** M = O Bond Dissociation

we will obtain a compact presentation of the computational results for about 25 systems that entails a relationship between the reaction energies on one hand and the activation barriers as well as the transition state structures on the other. Then we will demonstrate that the reaction energies of the systems studied correlate very well with the M–O bond dissociation energies (BDE) of the reactants (see Scheme 2).

**2. Systems and Methods**

We have carried out DF calculations<sup>26</sup> on the [2+3] cycloaddition of ethylene to various transition metal oxo compounds  $\text{MO}_3^q$  and  $\text{LMO}_3^q$  ( $q = -1, 0, 1$ ) with  $M = \text{Mo, W, Mn, Tc, Re, and Os}$  for different ligands  $L = \text{Cp, CH}_3, \text{Cl, and O}$  (see Table 1). The charge on the complexes  $\text{LMO}_3$  **1** was chosen such that the systems are isoelectronic to  $\text{OsO}_4$ ; the charge  $q$  on the fragments  $\text{MO}_3^q$  was varied to mimic the effect of various ligands  $L$  on the effective charge of that moiety. In light of previous results<sup>25</sup> we refrained from studying the formation of the diol from the metalladioxolane **2** or the [2+2] pathway. As motivation for our selection of systems, we briefly review the role of such compounds in the oxidation chemistry of olefins.

The oxo complexes of group VII (Mn, Tc, and Re) are of great interest for their propensity toward epoxidation and dihydroxylation.  $\text{MnO}_4^-$  is commonly used as a dihydroxylating agent<sup>37</sup> while the system  $\text{CH}_3\text{ReO}_3/\text{H}_2\text{O}_2$  is known to be an efficient epoxidation catalysts.<sup>13–18</sup> With regard to these two oxidation types of reactions, Tc takes a place in between.<sup>38</sup> Electronic and structural properties of Mn,<sup>39</sup> Tc,<sup>38</sup> and

(26) The DF routines were used as implemented in the program Gaussian94. Geometries were optimized without symmetry restrictions using the hybrid B3LYP approach, with effective core potentials and double- $\zeta$  basis sets, LanL2DZ, for the transition metals and 6-311G(d,p) basis sets for H, C, O, and F. For the final geometries, energies were calculated in single-point fashion with the metal basis set partly decontracted and augmented by one  $f$ -exponent. For related reactions, thermodynamic effects turned out to be of minor importance; since the present work aims at a comparative analysis, we refrained from applying correction terms, e.g. for zero-point energies.

(27) *Gaussian 94*, Revision D.4; Frisch, M. J. et al.; Gaussian, Inc.: Pittsburgh, PA, 1995.

(28) Becke, A. D. *J. Chem. Phys.* **1993**, *98*, 5648.

(29) Lee, C.; Yang, W.; Parr, R. G. *Phys. Rev. B* **1988**, *37*, 785.

(30) Hay, P. J.; Wadt, W. R. *J. Chem. Phys.* **1985**, *82*, 299.

(31) Krishnan, R.; Binkley, J.; Seeger, R.; Pople, J. *J. Chem. Phys.* **1980**, *72*, 650.

(32) McLean, A.; Chandler, G. *J. Chem. Phys.* **1980**, *72*, 5639.

(33) Frenking, G.; Antes, I.; Böhme, M.; Dapprich, S.; Ehlers, A. W.; Jonas, V.; Neuhaus, A.; Otto, M.; Stegmann, R.; Veldkamp, A.; Vyboishchikov, S. F. In *Reviews in Computational Chemistry*; Lipkowitz, K. B., Boyd, D. B., Eds.; VCH: New York, 1996; Vol. 8, p 63.

(34) Ehlers, A. W.; Böhme, M.; Dapprich, S.; Gobbi, A.; Höllwarth, A.; Jonas, V.; Köhler, K. F.; Stegmann, R.; Veldkamp, A.; Frenking, G. *Chem. Phys. Lett.* **1993**, *208*, 111.

(35) Gisdakis, P.; Antonczak, S.; Rösch, N. *Organometallics* **1999**, *18*, 5044.

(36) Marcus, R. A. *J. Phys. Chem.* **1968**, *72*, 891.

**Table 1.** Characteristics of Various Transition Metal Oxo Complexes **1**  $\text{LMO}_3^q$  and  $\text{MO}_3^q$  ( $q = -1, 0, 1$ ) with  $M = \text{Mo, W, Mn, Tc, Re, and Os}$  and  $L = \text{Cp, CH}_3, \text{Cl, and O}$  as Reactants of the [2+3] Cycloaddition of Ethylene: Reaction Energies  $\Delta E_0$  of the Formation of the Metalladioxolane **2**,  $\text{LMO}(\text{O}_2\text{C}_2\text{H}_4)$ , and  $\text{MO}(\text{O}_2\text{C}_2\text{H}_4)$ , the Corresponding Activation Barriers  $\Delta E^\ddagger$ , M–O Bond Dissociation Energies BDE of **1** (energies in kcal/mol), C–O Distances  $d$  (in Å) of the Transition States ( $\ddagger$ ) and the Products **2**, and Mulliken Charges  $q_M$  (in e) of the Metal Centers of **2** and of the Fragments **3**,  $\text{LMO}_2$ , and  $\text{MO}_2$

	$\Delta E_0$	$\Delta E^\ddagger$	BDE	$d^\ddagger$	$d(2)$	$q_M(2)$	$q_M(3)$
$\text{CH}_3\text{MnO}_3$	−34.3	8.9	100.1	2.087	1.430	0.94	0.82
$\text{MnO}_4^-$	−47.5	8.2	83.6	2.083	1.408	0.89	0.67
$\text{CpTcO}_3$	−38.9	5.5	84.8	2.150	1.427	0.98	0.86
$\text{CH}_3\text{TcO}_3$	0.7	23.7	131.3	1.935	1.443	1.18	1.04
$\text{ClTcO}_3$	−17.7	11.5	118.3	2.033	1.441	1.18	1.06
$\text{TcO}_4^-$	1.5	27.3	123.0	1.989	1.418	1.11	0.82
$\text{CpReO}_3^a$	−13.4	17.1	104.1	1.970	1.415	1.05	0.91
$\text{CH}_3\text{ReO}_3^a$	26.4	38.4	148.4	1.829	1.451	1.30	1.14
$\text{ClReO}_3^a$	10.0	25.8	132.3	1.888	1.451	1.27	1.12
$\text{ReO}_4^-$	26.0	40.2	133.1	1.801	1.424	1.21	0.92
$\text{CpMoO}_3^-$	6.6	34.2	133.0	1.834	1.408	1.02	0.71
$\text{CH}_3\text{MoO}_3^-$	40.1	54.1	164.5	1.740	1.417	0.95	0.59
$\text{ClMoO}_3^-$	30.2	45.1	153.1	1.781	1.421	1.03	0.71
$\text{CpWO}_3^-$	24.0	47.0	144.9	1.774	1.411	1.06	0.69
$\text{CH}_3\text{WO}_3^-$	63.2	69.6	175.4	1.667	1.424	0.88	0.61
$\text{ClWO}_3^-$	55.9	61.5	162.4	1.689	1.433	0.95	0.63
$\text{OsO}_4$	−18.1	12.0	108.5	2.126	1.446	1.49	1.61
$\text{MnO}_3^-$	8.4	36.9	146.0	1.855	1.411	0.51	0.12
$\text{TcO}_3^-$	32.0	52.7	173.0	1.774	1.406	0.58	0.15
$\text{TcO}_3$	−14.7	22.4	146.1	1.964	1.429	1.08	0.88
$\text{TcO}_3^{+b}$	−74.9		105.5		1.448	1.43	1.45
$\text{ReO}_3^-$	68.5	72.5	185.1	1.692	1.423	0.53	0.22
$\text{ReO}_3$	14.9	37.3	157.5	1.851	1.454	1.11	0.89
$\text{ReO}_3^{+b}$	−45.3		122.3		1.487	1.48	1.48
$\text{MoO}_3^-$	33.6	56.0	165.8	1.757	1.413	0.61	0.10
$\text{MoO}_3$	−8.9	24.6	143.8	1.933	1.436	1.11	0.81
$\text{WO}_3$	1.6	37.2	136.8	1.849	1.465	1.00	0.76

<sup>a</sup> Note that the calculated Re–O bond dissociation energies differ from those presented earlier where two  $f$ -exponents have been used at the Re center instead of only one  $f$ -exponent<sup>34</sup> as in the present study.

<sup>b</sup> Transition state could not be located.

$\text{Re}^{40–42}$  compounds have previously been analyzed in various DF studies. Differences in reactivity between analogous Tc and Re oxo compounds have been attributed to relativistic effects on the Lewis acidity and the polarizability of the  $\text{MO}_3$  moiety;<sup>40–42</sup> Re was found to form a stronger and harder (less polarizable) Lewis acid center than Tc.  $\text{CpReO}_3^{43–46}$  has been shown to react with olefins to form dioxylates

(37) March, J. *Advanced Organic Chemistry*, 3rd ed.; Wiley: New York, 1985; p 732.

(38) Herrmann, W. A.; Alberto, R.; Kiprof, P.; Baumgärtner, F. *Angew. Chem., Int. Ed. Engl.* **1990**, *29*, 189.

(39) Dickson, R. M.; Ziegler, T. *Int. J. Quantum Chem.* **1996**, *58*, 681.

(40) Köstlmeier, S.; Häberlen, O. D.; Rösch, N.; Herrmann, W. A.; Solouki, B.; Bock, H. *Organometallics* **1996**, *15*, 1872.

(41) Köstlmeier, S.; Pacchioni, G.; Rösch, N. *J. Organomet. Chem.* **1996**, *514*, 111.

(42) Köstlmeier, S.; Nasluzov, V. A.; Herrmann, W. A.; Rösch, N. *Organometallics* **1997**, *16*, 1786.

(43) Burrell, A. K.; Cotton, F. A.; Daniels, L. M.; Petricek, V. *Inorg. Chem.* **1995**, *34*, 4253.

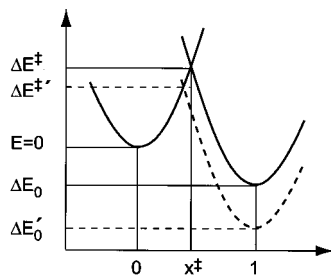


**Figure 1.** Schematic representation of a reaction profile  $E(x)$  along a generalized reaction coordinate  $x$  with the reaction barrier  $\Delta E^\ddagger$  at the transition state  $x^\ddagger$ .

(Scheme 1).<sup>47–49</sup> In the present study, the complex  $\text{CH}_3\text{MnO}_3$ , which has not been characterized experimentally, was included for comparison with analogous Tc and Re compounds, although it had been predicted to be unstable on the basis of Hartree–Fock results.<sup>50</sup> With the DF approach employed here, we found the Cp ligand to be bound to the Mn center in  $\eta^1$  and not in  $\eta^5$  fashion; therefore, we excluded the complex from the present systematic comparison.

Besides MTO/ $\text{H}_2\text{O}_2$ , also molybdenum and tungsten peroxo complexes are known to be oxygen transfer catalysts, i.e., they epoxidize olefins.<sup>20,21</sup> To the best of our knowledge there are no experimental studies available which investigate the capability of Mo and W oxo compounds to undergo a [2+3] cycloaddition.<sup>51</sup> Nevertheless, to broaden our study of [2+3] cycloaddition by oxo compounds, we also included Mo and W complexes.

In the following, we will use the Marcus equation, originally derived for electron-transfer reactions,<sup>36</sup> to relate the activation barriers  $\Delta E^\ddagger$  of ethylene [2+3] cycloaddition to a complex  $\text{LMO}_3$  to the corresponding reaction energy  $\Delta E_0$ . The Marcus approach has been successfully applied to many chemical reactions,<sup>52,53</sup> also in a generalized multidimensional version,<sup>54</sup> but failures have also been reported.<sup>54,55</sup> Most applications dealt with reactions of organic compounds, also with results obtained from ab initio calculations.<sup>55,56</sup> Marcus theory starts from a general schematic reaction profile (see Figure 1): two parabolas for reactants and products along a formal reaction coordinate  $x$  that ranges from 0 to 1. Assuming the same parabola curvatures for reactants and products, straightforward algebra leads to the desired result:

$$\Delta E^\ddagger = \Delta E_0^\ddagger + \frac{1}{2} \Delta E_0 + \frac{1}{16\Delta E_0^\ddagger} \Delta E_0^2 = \Delta E_0^\ddagger \left( 1 + \frac{\Delta E_0}{4\Delta E_0^\ddagger} \right)^2 \quad (1)$$

$$x^\ddagger = \frac{1}{2} \left( 1 + \frac{\Delta E_0}{4\Delta E_0^\ddagger} \right) \quad (2)$$

The intrinsic reaction barrier  $\Delta E_0^\ddagger$ , the central parameter of Marcus theory, represents the barrier of a thermoneutral reaction ( $\Delta E_0 = 0$ ) where the transition state is located midway between reactants and products, at  $x^\ddagger = 1/2$ . According to the Marcus equation, endothermic reactions ( $\Delta E_0 > 0$ ) feature larger barriers ( $\Delta E^\ddagger > \Delta E_0^\ddagger$ ) and exothermic reactions feature smaller barriers ( $\Delta E^\ddagger < \Delta E_0^\ddagger$ ) (Figure 1).

(44) Herrmann, W. A.; Serrano, R.; Bock, H. *Angew. Chem., Int. Ed. Engl.* **1984**, *23*, 383.

(45) Klahn-Oliva, A. H.; Sutton, D. *Organometallics* **1984**, *3*, 1313.

(46) Kühn, F. E.; Herrmann, W. A.; Hahn, R.; Elison, M.; Blümel, J.; Herdtweck, E. *Organometallics* **1994**, *13*, 1601.

(47) Gable, K. P.; Phan, T. N. *J. Am. Chem. Soc.* **1994**, *116*, 833.

(48) Gable, K. P.; Juliette, J. J. *J. Am. Chem. Soc.* **1995**, *117*, 955.

(49) Gable, K. P.; Juliette, J. J. *J. Am. Chem. Soc.* **1996**, *118*, 2625.

(50) Szyperski, T.; Schwerdtfeger, P. *Angew. Chem., Int. Ed. Engl.* **1989**, *28*, 1228.

(51) Arzoumanian, H. *Coord. Chem. Rev.* **1998**, *178–180*, 191.

(52) Albery, W. J. *Annu. Rev. Phys. Chem.* **1980**, *31*, 227.

(53) (a) Murdoch, J. R. *J. Am. Chem. Soc.* **1983**, *105*, 2667. (b) Chen, M.; Murdoch, J. R. *J. Am. Chem. Soc.* **1984**, *106*, 4735.

(54) Guthrie, J. P. *J. Am. Chem. Soc.* **1996**, *118*, 12878. (b) Guthrie, J. P. *J. Am. Chem. Soc.* **2000**, *122*, 5529.

(55) Guthrie, J. P. *Can. J. Chem.* **1996**, *74*, 1283 and references therein.

(56) (a) Lee, W. T.; Masel, R. I. *J. Phys. Chem.* **1996**, *100*, 10945. (b) Lee, W. T.; Masel, R. I. *J. Phys. Chem.* **1998**, *102*, 2332.

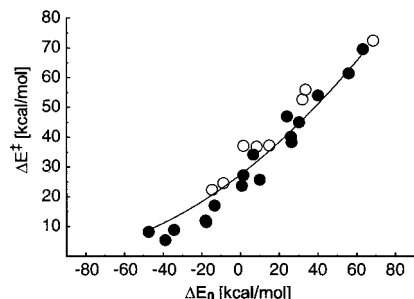


**Figure 2.** Activation energies  $\Delta E^\ddagger$  of ethylene [2+3] cycloaddition to complexes  $\text{LMO}_3$  (filled circles) and fragments  $\text{MO}_3^q$  ( $q = -1, 0, 1$ ) (empty circles) as a function of the reaction energy  $\Delta E_0$ . Also shown is the parabola according to Marcus theory (solid line) with  $\Delta E_0^\ddagger = 27.5$  kcal/mol fitted to all data of Table 1 according to eq 1. All energies in kcal/mol.

### 3. Results and Discussion

In Table 1 we present pertinent calculated quantities that characterize various transition metal oxo complexes **1**  $\text{LMO}_3^q$  and  $\text{MO}_3^q$  ( $q = -1, 0, 1$ ) with  $M = \text{Mo, W, Mn, Tc, Re, and Os}$  and  $L = \text{Cp, CH}_3, \text{Cl, and O}$  as reactants of the [2+3] cycloaddition of ethylene: the reaction energy  $\Delta E_0$  of the formation of the metalladioxolane **2**,  $\text{LMO}(\text{O}_2\text{C}_2\text{H}_4)$ , and  $\text{MO}(\text{O}_2\text{C}_2\text{H}_4)$ , the corresponding activation barriers  $\Delta E^\ddagger$ , the M–O bond dissociation energies BDE of **1**, the C–O distances  $d$  of the transition states ( $\ddagger$ ) and of the products **2**, as well as Mulliken charges  $q_M$  of the metal centers of **2** and of the fragments **3**,  $\text{LMO}_2$ , and  $\text{MO}_2$ . These data are in good agreement with previously published results.<sup>4–7,24,25</sup>

The activation barriers of the complexes of Mn, Tc, and Re exhibit several interesting trends. For a given ligand type L, the barrier height increases with the atomic number of the metal center. For  $\text{MO}_4^-$  ( $M = \text{Mn, Tc, Re}$ ) the barrier heights are 8.2, 27.3, and 40.2 kcal/mol, respectively, and for  $\text{CH}_3\text{MO}_3$  they are 8.9, 23.7, and 38.4 kcal/mol; for  $\text{CpMO}_3$  the barriers are 5.5 and 17.1 kcal/mol for  $M = \text{Tc}$  and  $\text{Re}$ , respectively. For each metal center, the barrier heights of the two complexes  $\text{MO}_4^-$  and  $\text{CH}_3\text{MO}_3$  are quite close. For  $M = \text{Tc}$  and  $\text{Re}$ , substitution of the methyl group of  $\text{CH}_3\text{MO}_3$  by a Cp ligand reduces the barrier significantly, by 18.2 and 21.3 kcal/mol, respectively. For the complexes  $\text{LMO}_3^-$  ( $M = \text{Mo}$  and  $\text{W}$ ) the change of the barriers due to the corresponding (formal) ligand replacement is similar in size, but all barriers are quite a bit larger than their Tc and Re analogues. For  $\text{OsO}_4$ , we find a rather small barrier, in agreement with previous investigations.<sup>4–7</sup>

In Figure 2 we show for the complexes  $\text{LMO}_3^q$  and  $\text{MO}_3^q$  studied how the activation energies  $\Delta E^\ddagger$  of the [2+3] cycloaddition of ethylene depend on the reaction energies  $\Delta E_0$ . From a least-squares fit of the data for the ligated complexes to eq 1, one derives an intrinsic reaction barrier  $\Delta E_0^\ddagger$  of 25.1 kcal/mol (Figure 2), with a mean absolute deviation of 3.2 kcal/mol. This barrier value is close to the calculated barrier height of  $\text{CH}_3\text{-TcO}_3$ , 23.7 kcal/mol, where the reaction energy is 0.7 kcal/mol (Table 1). The overall success of the compact representation of activation energies by the Marcus equation becomes quite impressive if one takes into account that the barriers span the wide range from about 5 to 70 kcal/mol. It is important to note that the ligand-free fragments  $\text{MO}_3^q$  ( $q = -1, 0, 1$ ) obey essentially the same relationship as the ligated complexes; the mean absolute deviation from the Marcus estimate based on the ligated compounds is only 4.3 kcal/mol. A fit over all data of Table 1 (ligated and fragment compounds) yields  $\Delta E_0^\ddagger = 27.5$  kcal/mol with a mean absolute deviation of 3.9 kcal/mol.

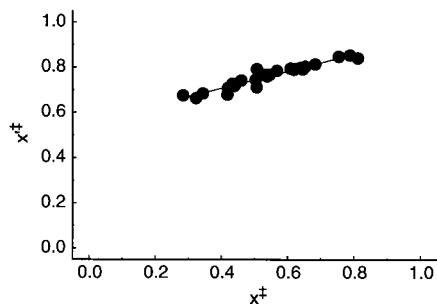


**Figure 3.** Location  $x^{\ddagger}$  of the transition state along the reaction coordinate  $x' = d(\mathbf{2})/d(\text{C}-\text{O})$  as a function of the formal Marcus reaction coordinate  $x^{\ddagger}$  according to eq 2.  $d(\mathbf{2})$  is the length of the newly formed C–O bond of the metalladioxolane **2** and  $d(\text{C}-\text{O})$  is the length of that bond during the reaction.

These findings strongly suggest that the ligand L affects the barrier of ethylene [2+3] addition to LMO<sub>3</sub> essentially by a modulation of the charge of active MO<sub>3</sub> (see below).<sup>56</sup>

The formal reaction coordinate  $x$  of Marcus theory is not easy to identify. Nevertheless, it is often useful to order the structures of the various transition states. For this purpose, one may select the ratio  $x'$  of the C–O distances  $d$  of the product **2** and of any intermediate structures,  $x' = d(\mathbf{2})/d(\text{C}-\text{O})$ . This definition of the reaction coordinate exhibits the proper asymptotic values,  $x' = 0$  for the reactants and  $x' = 1$  for the products. For this approximation of the reaction coordinate, it seems natural to associate the parabola of the reactant section of the reaction profile (Figure 1) with the M–O stretching mode, while the product section may be related to the C–O stretching mode in the corresponding metalladioxolane. Given the success of Marcus theory for the present set of reactions (Figure 2), one may well wonder how closely the underlying assumption holds that both parabolic sections of the reaction profile exhibit the same curvature (see eq 1). As an example, we mention that the symmetric (861 cm<sup>-1</sup>) and asymmetric (980 cm<sup>-1</sup>) C–O stretching modes of the dioxylate complex derived from CH<sub>3</sub>-ReO<sub>3</sub> are characterized by force constants of 8.2 and 9.1 mdyne/Å, respectively. The average force constant, 8.7 mdyne/Å, is indeed quite close to the force constant values of the M–O stretching modes of CH<sub>3</sub>ReO<sub>3</sub>, 8.9 mdyne/Å, with frequencies of 993 cm<sup>-1</sup>. Moreover, Figure 3 demonstrates that the location of the transition state,  $x^{\ddagger} = d(\mathbf{2})/d^{\ddagger}(\text{C}-\text{O})$ , varies linearly with the quantity  $x^{\ddagger}$  as given by eq 2 and thus on the reaction energy  $\Delta E_0$ , just as the values  $x^{\ddagger}$  of the formal reaction coordinate  $x$  of Marcus theory do. However, for a thermoneutral reaction,  $x^{\ddagger}$  does not acquire the value  $1/2$  of  $x^{\ddagger}$ . For practical purposes, e.g. for estimating the location of transition structures,  $x^{\ddagger}$  is a convenient measure.

Thus far, we have shown that Marcus theory provides a convenient compact representation of the energetics of the ethylene [2+3] cycloaddition to a large class of transition metal oxo complexes LMO<sub>3</sub><sup>q</sup>. Now, we proceed to an analysis of this relationship.

Previously we have found<sup>35</sup> that the Re–O bond strength in various complexes LReO<sub>3</sub> is affected by two factors: (i) the  $\sigma$  donor–acceptor interaction between moieties L<sup>-</sup> and ReO<sub>3</sub><sup>+</sup> as measured by the corresponding frontier orbital energy gap and (ii) the difference of the capabilities of the reactants LReO<sub>3</sub> **1** and the products LReO<sub>2</sub> **3** (Scheme 2) to stabilize electron charge density on the metal center. Interestingly, the first factor alone fails to provide a rationalization of the ordering of BDEs among the various complexes.<sup>35</sup> The  $\sigma$  accepting orbital of the fragment ReO<sub>3</sub> that interacts with the pertinent  $\sigma$  orbital of the donor L is  $\pi$  antibonding with respect to the Re–O bond;

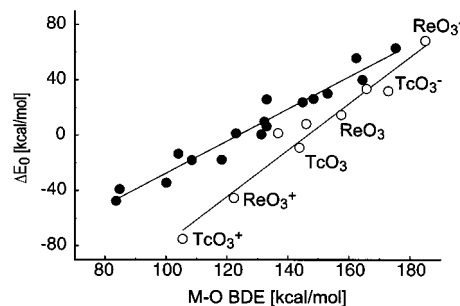


**Figure 4.** Reaction energy  $\Delta E_0$  of ethylene [2+3] cycloaddition to the precursor complexes LMO<sub>3</sub> (filled circles) and fragments MO<sub>3</sub><sup>q</sup> ( $q = -1, 0, 1$ ) (empty circles) as a function of the M–O bond dissociation energy (BDE) of these precursors **1**. Energies in kcal/mol.

therefore, stronger donors L are expected to result in weaker Re–O bonds. By varying the charge of the fragment ReO<sub>3</sub><sup>q</sup> ( $q = 1, 0, -1$ ) we are able to model the effect of the ligand L on the charge of the ReO<sub>3</sub> moiety, illustrating the effect. The Re–O bonds elongate along the series, with 1.690, 1.712, and 1.737 Å for  $q = 1, 0, -1$ , respectively. However, the Re–O BDEs of ReO<sub>3</sub><sup>q</sup> exhibit the opposite trend, 122.3, 157.5, and 185.1 kcal/mol, respectively (longer but stronger bonds, see Table 1). Therefore, a second counteracting factor has to be at work, namely the difference in electron affinities (EA) of the moieties ReO<sub>3</sub><sup>q</sup> and ReO<sub>2</sub><sup>q</sup>:<sup>35</sup> the larger fragment ReO<sub>3</sub> is able to stabilize additional charge better than the smaller moiety ReO<sub>2</sub> (EA: ReO<sub>3</sub><sup>+</sup> 10.8 eV, ReO<sub>2</sub><sup>+</sup> 9.2 eV, ReO<sub>3</sub> 3.6 eV, ReO<sub>2</sub> 2.4 eV). Ultimately, LReO<sub>3</sub> compounds with a higher electron density on the metal fragment ReO<sub>3</sub> (due to the better  $\sigma$  donor L) have stronger Re–O bonds.

Both reactions, the addition of an olefin to a LMO<sub>3</sub> moiety (Scheme 1) and the abstraction of an oxygen atom from the LMO<sub>3</sub> moiety (Scheme 2), feature a formal two-electron reduction of the metal center. Therefore, one expects a similar behavior of the corresponding reaction energies  $\Delta E_0$  and M–O bond dissociation energies BDE (see Figure 4). Both groups, ligated complexes LMO<sub>3</sub><sup>q</sup> and ligand-free species MO<sub>3</sub><sup>q</sup>, separately exhibit linear trends: complexes with higher M–O BDE show less exothermic or even endothermic reaction energies of the [2+3] cycloaddition. The reaction energies  $\Delta E_0$  cover substantial ranges (Table 1), from -47.5 (MnO<sub>4</sub><sup>-</sup>) to 63.2 kcal/mol (CH<sub>3</sub>WO<sub>3</sub><sup>-</sup>) for the ligated complexes LMO<sub>3</sub><sup>q</sup> and from -74.9 (TcO<sub>3</sub><sup>+</sup>) to 68.5 kcal/mol (ReO<sub>3</sub><sup>-</sup>) for the ligand-free fragments MO<sub>3</sub><sup>q</sup>. The M–O dissociation energies exhibit similarly strong variations, between 83.6 and 175.4 kcal/mol for the ligated complexes and between 105.5 and 185.1 kcal/mol for the fragments (Table 1). For a specific ligand L, the M–O BDE of LMO<sub>3</sub> increases with the atomic number of the metal center along the series Mn, Tc, Re (Table 1). Concomitantly, the charge separation of the M–O bond also increases, rendering the bond increasingly more ionic. For instance, the M–O BDE values of CH<sub>3</sub>MO<sub>3</sub> are 100.1, 131.3, and 148.4 kcal/mol for M = Mn, Tc, and Re, respectively, while the corresponding M–O charge differences are 1.14, 2.19, and 2.63 e.

The fragment ReO<sub>3</sub><sup>+</sup> has a lower M–O BDE than the more electron rich fragments ReO<sub>3</sub> and ReO<sub>3</sub><sup>-</sup>. The same trend holds for the series TcO<sub>3</sub><sup>q</sup>, with the Tc–O dissociation energies shifted to lower energies by 12–17 kcal/mol. This reflects the fact that the smaller fragments TcO<sub>3</sub><sup>q</sup> feature lower electron affinities than the corresponding species ReO<sub>3</sub><sup>q</sup> (EA: TcO<sub>3</sub><sup>+</sup> 10.6 eV, TcO<sub>2</sub><sup>+</sup> 8.9 eV; TcO<sub>3</sub> 3.2 eV, TcO<sub>2</sub> 2.0 eV; see above).

To put the energy of the two reduction reactions (Schemes 1 and 2) on a more quantitative footing, we compare the partial

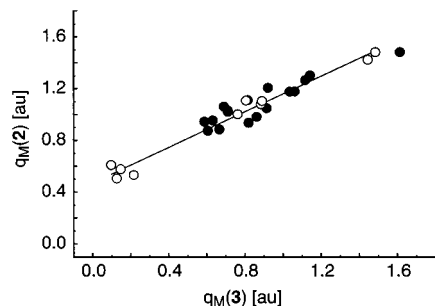


**Figure 5.** Correlation between the Mulliken charges (in e) of the metal centers of the dioxofragments **3**,  $\text{LMO}_2$ , and  $\text{MO}_2^q$ , and of the metalladioxolane intermediates **2**,  $\text{LMO}(\text{O}_2\text{C}_2\text{H}_4)$ , and  $\text{MO}(\text{O}_2\text{C}_2\text{H}_4)^q$ . Data for systems with and without a ligand L are indicated by filled and empty circles, respectively.

charges of the metal centers of the products of both reactions **2** and **3** (Table 1). Inspection of Figure 5 shows that the Mulliken charges on the metal centers of  $\text{LMO}(\text{O}_2\text{C}_2\text{H}_4)$  **2** and  $\text{LMO}_2$  **3** exhibit a satisfactorily linear correlation, indicating a similarity of the configurations of the metal centers of both product complexes **2** and **3**. Comparison of the metal charges  $q_{\text{M}}(\mathbf{2})$  of  $\text{LMO}_3^q$  and  $\text{MO}_3^q$  to  $q_{\text{M}}(\mathbf{3})$  of  $\text{LMO}_2^q$  and  $\text{MO}_2^q$  shows that the metal centers of the smaller fragments feature smaller positive partial charges. Thus, M–O bonds of the systems  $\text{LMO}_3^q$  are more polarized, exhibiting an increased ionic contribution to the metal–oxygen interaction.

#### 4. Conclusion

The M–O dissociation energies of the metal oxo complexes  $\text{LMO}_3$  **1** are easily calculated. Via the approximate linear

correlation (Figure 5) of these bond energies with the reaction energies  $\Delta E_0$  of the ethylene [2+3] cycloaddition at these metal complexes (Scheme 1) we are not only able to predict this reaction energy from the BDE of similar oxo complexes, but we can also estimate the activation barriers  $\Delta E^\ddagger$  of the [2+3] cycloaddition via the Marcus equation (Figure 2). Complexes  $\text{LMO}_3^q$  ( $q = -1, 0, 1$ ) with a lower M–O BDE feature a more exothermic cycloaddition reaction and thus a lower activation barrier  $\Delta E^\ddagger$ . The relationships discussed hold to a very good approximation over a broad range of systems  $\text{LMO}_3^q$  with  $\text{M} = \text{Mo}, \text{W}, \text{Mn}, \text{Tc}, \text{Re}, \text{Os}$  and  $\text{L} = \text{Cp}, \text{CH}_3, \text{Cl}, \text{O}$ , also for different charges  $q$ . The reason for the correlation between M–O BDE and  $\Delta E_0$  is based on the fact that both reactions are controlled by the ability of the metal center to be reduced.

The intrinsic reaction barrier  $\Delta E_0^\ddagger$  of a thermoneutral olefin [2+3] cycloaddition was found to be quite high: 25.1 kcal/mol for the ligated complexes and 27.5 kcal/mol for all compounds studied (i.e. including the ligand-free model systems). Thus, the experimentally known olefin dihydroxylation reactions of the complexes  $\text{OsO}_4$  and  $\text{MnO}_4^-$  (with low calculated barriers ( $\Delta E^\ddagger$ ) of 12.0 and 8.2 kcal/mol, respectively) are feasible due to their large exothermicities ( $\Delta E_0$ ) of  $-18.1$  and  $-47.5$  kcal/mol, respectively (Figure 1).

**Acknowledgment.** We thank K. M. Neyman, J. Rak, and A. A. Voityuk for stimulating discussions. This work has been supported by the Deutsche Forschungsgemeinschaft and the Fonds der Chemischen Industrie.

JA0026915